Eur. Phys. J. D **44**, 227–231 (2007)
DOI: 10.1140/epjd/e2007-00005-1

THE EUROPEAN PHYSICAL JOURNAL D

Inertial fusion research in China

X.T. He[a] and W.Y. Zhang

National Hi-Tech Inertial Confinement Fusion Committee, P.O. Box 8009-55, Beijing 100088, P.R. China

Received 3rd January 2006 / Received in final form 28 July 2006
Published online 17 January 2007 –

Abstract. The goal of the first milestone of the inertial fusion program in China is to reach fusion ignition and plasma burning in about 2020. Under the program, in the past years, the inertial fusion physics research achieved great progress; the laser facilities and the support technologies for laser drivers are advanced; the advanced diagnostic techniques are developed and the relatively integrated system is set up; the precise target fabrications are coordinately developed.

PACS. 52.38.Kd Laser-plasma acceleration of electrons and ions – 52.38.Fz Laser-induced magnetic fields in plasmas

1 Introduction

The inertial fusion program under National Hi-Tec Inertial Confinement Fusion Committee in China has been performed since 1993, the key institutions to join the program are the Laser Fusion Research Center of China Academy of Physics Engineering; Institute of Applied Physics and Computational Mathematics; National Laboratory on High Power Laser and Physics; China Institute of Atomic Energy. In addition, Institute of Physics of Chinese Academy of Sciences (CAS) and Shanghai Institute of Fine Optics and Mechanics of CAS, and some universities join the program as well. The mission of the program is to study and understand inertial fusion physics and to develop the drivers, the goal is toward ignition and plasma burning in about 2020, for this purpose, hence, to coordinately develop driver technologies and architectures, precision measurements and relevant diagnostic systems, and precision target fabrications.

The emphases of this paper are given on the latest advances of inertial fusion physics and drivers, and the future plan for inertial fusion research and development in China.

2 Development of drivers

For the development of drivers involving lasers and Z-pinch, solid state laser facilities (Shenguang–SG series) are put to the first priority.

After SG-I was decommissioned in 1994, SG-II (Fig. 1a) that has eight beams and routine energy output of $\geq$6 kJ (1ω) and $\geq$3 kJ (3ω), is operating in high beam quality and has provided about thousands shots for experiments since 2000 [1]. This facility is the first successful development of two sets of double-pass and co-axial array main amplifier with the aperture of $\phi = 200$ mm for each beam.

Fig. 1. (a) SG-II laser bay and target chamber, (b) the ninth laser beam to be PW laser.

In addition to eight beams of SG-II, a new laser beam (named ninth beam) in Figure 1b, with laser energy output of 4.5 kJ (1ω) and 2.2 kJ (2ω), pulse duration 3 ns, began operating in the end of 2004 and is coupling with SG-II to be used as a diagnostic beam, such as X-ray backlighting, etc.

SG-IIU that is an upgraded SG-II and has laser energy output of 18 kJ (3ω), pulse duration 3 ns, will be operating in 2007.

[a] e-mail: xthe@iapcm.ac.cn

Fig. 2. SG-III prototype.

The ninth beam will also be set up as a petawatt laser (PW laser) with laser energy of 1–2 kJ, pulse duration of 1–2 picosecond, and be operating in 2007.

SG-III prototype with eight beams (Fig. 2), which is one of the eight bundles of SG-III and is of laser energy output of 15–20 kJ (3ω) serving for both technological platform of SG-III construction and physical experiment [2], began operating in 2005. The facility uses the most advanced technologies, such as a whole optical fiber front end and whole solid state laser pumping, etc.

SG-III laser facility will be used to investigate target physics before ignition for both direct-drive and indirect-drive ICF and will be operating in about 2010. The design has been completed and the support technologies are advanced. The facility has 64 beams (eight bundles) and laser energy output of 150–200 kJ (3ω) for a pulse duration of about 3 ns. If fast ignition is workable, SG-III will couple with PW laser of tens kJ to demonstrate fast ignition.

The project to architect SG-IV, National Ignition Driver (NID), that has laser energy output of about 1–1.5 MJ serving for the central ignition with moderate gain and fast ignition with high gain, has been authorized, and the architecture of SG-IV will be completed in about 2020.

In addition, KrF excimer laser facility and Z-Pinch device are developed as well in China.

3 The latest advances in target physics

(1) In the past ten years, the LARED series of codes that consists of the 2D and 3D codes has been developed and is currently checked by experiments on SG-II. The series cover 2D code for hydrodynamics and 3D code for radiation transport; 2D codes for direct-drive and indirect-drive implosion dynamics, ignition and burning propagation; 2D and 3D codes for hydrodynamic instabilities and implosion dynamics; 2D and 3D for particle simulation; and others. It has been applied to investigate hohlraum physics, radiation transport, direct-drive and indirect-drive implosion dynamics, hydrodynamic instabilities, thermonuclear ignition and plasma burning and laser-plasma interactions, and so on.

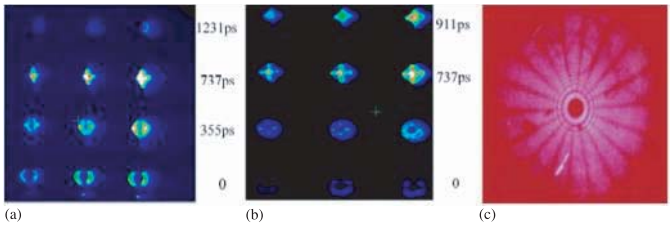

Fig. 3. (a) and (b) Capsule implosion dynamic framing, (c) particle encoding image.

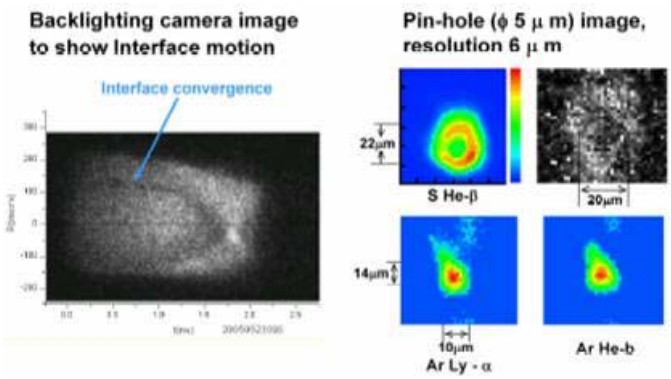

Fig. 4. Dynamic process of interface between inner wall of capsule shell and fuel region.

(2) Implosion dynamics studies on SG-II facility and numerical simulations using LARED series.

Direct-drive implosion experiments on SG-II have obtained many important data involving the capsule dynamics framing image and encoding image of the particles escaping from the compressed fuel region, as seen in Figure 3, etc.

Indirect-drive implosion experiments on SG-II have observed many important results involving hohlraum behavior, fuel core framing and self-backlighting images, etc. In particular, we have precisely measured the dynamic process of the interface between capsule shell (doped sulphur thin film on the inner wall) and fuel region (doped argon) using X-ray backlighting and pin-hole images with the resolution of 6 μm, see Figure 4, it contributes to our understanding of implosion dynamics and checking of LARED series.

The LARED simulations reproduced the indirect-drive experimental results of the capsule implosion compression, and the experimental profiles of the imploding fuel core, which vary with the length L of the hohlraum, agree with numerical simulations, see Figure 5.

(3) The radiation transport experiments have measured the transport time, energy spectrum structures, and heat wave propagation in the low density foam.

(4) Equation of state (EOS) in high pressure is precisely measured using SG-II laser to irradiate aluminium-copper impedance-matched planar targets (Fig. 6a) and 23 Mbar for copper with velocity accuracy less than 2% is

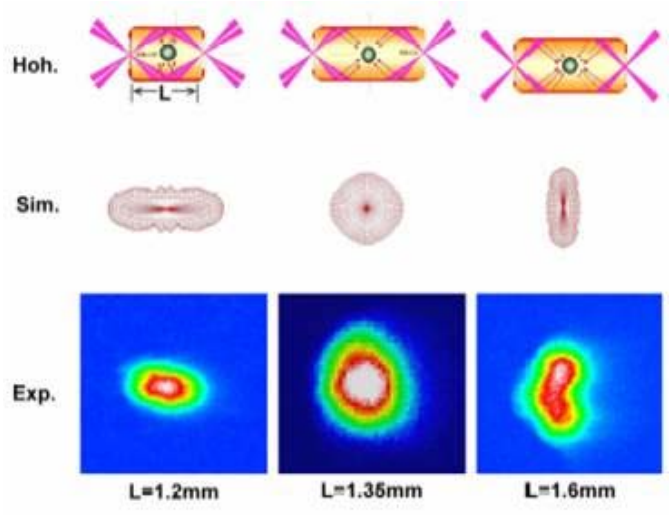

Fig. 5. Experimental and theoretical comparison of the fuel core profiles in indirect-drive implosion.

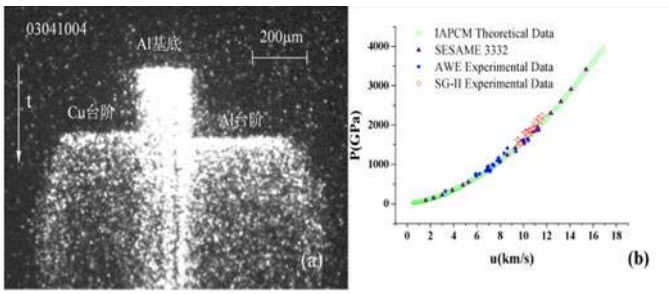

Fig. 6. Plots for measurements of EOE: (a) aluminium-copper impedance-matched target shock wave recorded by streak camera with velocity accuracy less than 2%, (b) experimental and theoretical curves.

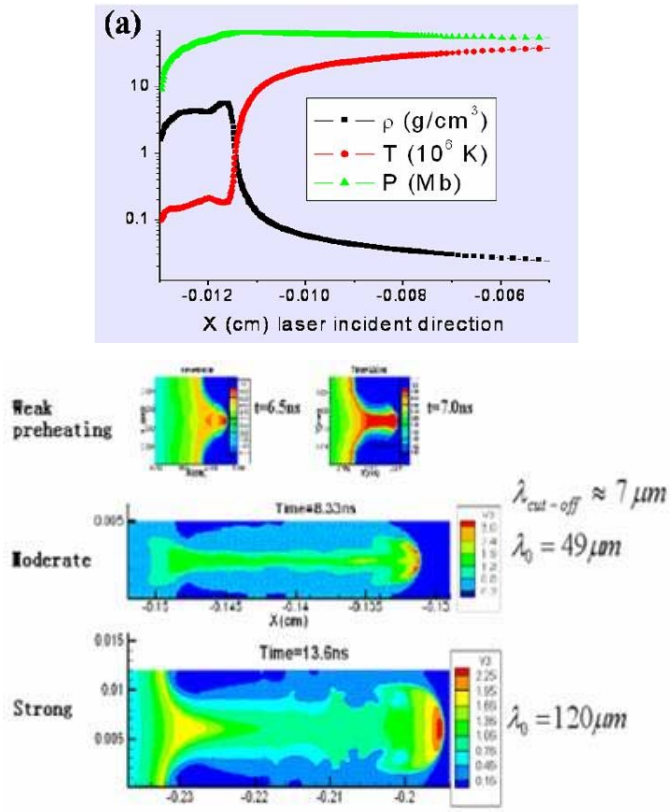

Fig. 7. (a) Background: a typical simulated 1D profiles of density, temperature and pressure nearby the ablative front. There may have a small temperature tongue from non-local heat conduction at ablative front. (b) Long jet generated by ablative Rayleigh-Taylor (RT) instability.

obtained. The experimental results on SG-II and the theoretical simulations are shown in Figure 6b, where other experiments are also compared.

(5) Hydrodynamic instabilities may occur at an interface between two fluids with different densities when a perturbation exists. Ablation hydrodynamic instability occurs at a sharp ablation front (Fig. 7a), which is formed when a laser beam is incident on a target surface where the nonlinear heat conduction penetrates into over critical density. At that time, a small temperature tongue, i.e., preheating, exists ahead of the sharp ablation front due to X-ray emission from high temperature plasma and/or nonlocal heat conduction. We write the heat conductivity in the form of $\kappa = \kappa_{sh} h f$, where κ_{sh} is Spitzer-Harm conductivity, h is the flux limitation, $f = 1 + a/T + b/T^{3/2}$ and temperature T in units of 10^6 K, $b = 1$ and $c = 0.3$ (weak preheating), $b = 10$ and $c = 1$ (moderate), $b = 100$ and $c = 10$ (strong). Numerical simulations by LARED codes show that the weak preheating can adequately suppress the Kelvin-Helmholtz (KH) instability and thus leads to the spike formation without mushroom structure, however, the weak preheating cannot suppress the harmonic mode that results in the rupture of the spike due to interaction of the master mode with the harmonic mode. Enhancing the preheating still further, the moderate preheating can adequately suppress both KH instability and harmonic instability, as a result, the ablative Rayleigh-Taylor instability drives the formation of the long jets [3], see Figure 7b. It may contribute to understand some processes in inertial fusion and astrophysics.

(6) Fast ignition investigation by numerical simulations.

The implosion dynamics of the cone target is investigated by numerical simulations using LARED-S code under SG-IIU condition. The laser energy of 10 kJ is incident on the surface of the cone target capsule. After a laser pre-pulse power rising linearly from $W_0(t = 0) = 0$ to $W_1(t = 3.45\ \text{ns}) = 0.54 \times 10^{11}\ \text{W/cm}^2$, the laser power rises linearly from W_1 to $W_2 = 10^{13}\ \text{W/cm}^2$ at $t_2 = 4.2$ ns, and then keeps a constant W_2 till $t_3 = 4.9$ ns, at last, reduces to zero at $t_4 = 5.2$ ns. The capsule of the cone target has a CD shell with density of 1.0 g/cc, and the initial radius of the capsule is 325 μm. The cone makes an outer angle of 60 degree and the cone wall consists of copper.

The numerical results show that during implosion process the maximal density of the CD shell reaches over 1000 g/cc (Fig. 8a) and jets-like due to nonlinear RT instability are observed (10b). The implosion dynamics in

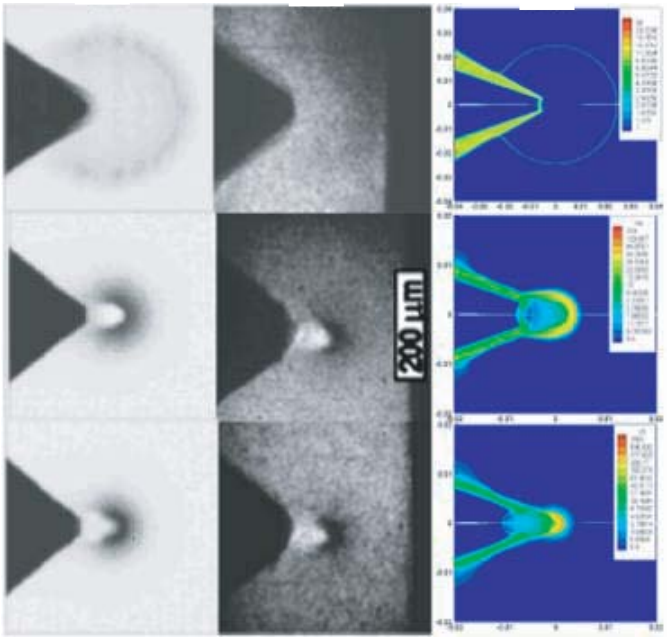

Fig. 8. Implosion dynamics of the cone target in different times from top to bottom: (a) experiment on OMEGA, (b) numerical simulation by LASNEX, (c) numerical simulation by LARED-S.

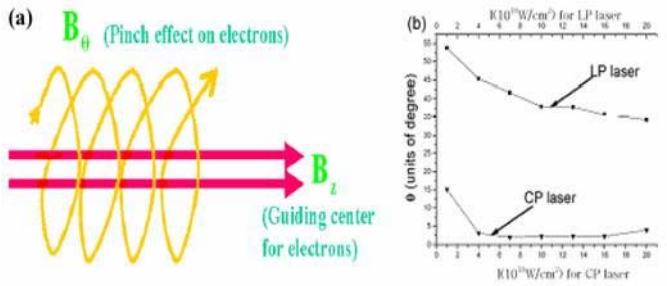

Fig. 9. Collimation of electrons: (a) magnetic field effects, (b) divergent angles.

our case is compared with experiment on OMEGA laser facility and numerical simulation by LASNEX, and the profiles agree very well.

The collimation and the stabilization of the relativistic electron beam (REB) in PW laser interaction with relativistic plasma are one of the critical issues for fast ignition. Numerical simulations using 3D-PIC (one of LARED series) show that the circularly polarized (CP) laser interaction with dense plasma generates both axially and azimuthally magnetic fields, the azimuthal field causes a pinch effect on REB and the axial field plays a trapping role that leads to REB having a small divergent angle, such as 2–3° for laser intensity of 10^{19} W/cm^2. On the other hand, the linearly polarized (LP) laser interaction with dense plasma generates only azimuthally magnetic field that leads to the REB having a large divergent angle, such as about 30–40° for laser intensity 2×10^{19} W/cm^2, as shown in Figure 9. Moreover, the transverse spot of

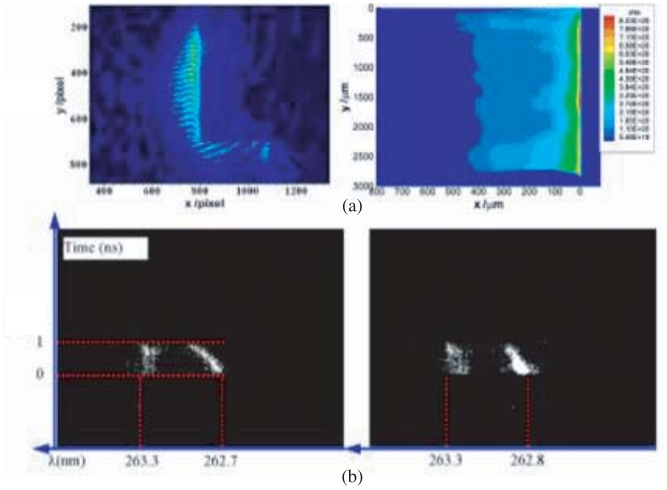

Fig. 10. (a) The dynamic interferogram image (left) of soft X-ray laser with wavelength 13.9 nm and the reconstructed electronic density of CH plasma near critical surface at the time of 1 ns after the peak of the drive laser intensity (right). (b) The patterns from Thomson scattering experiment.

the electric current exhibits an ellipse-like structure as the REB penetrating dense plasma deeply, therefore, when the REB separating from the LP laser beam penetrates the overdense plasma where the REB deposits energy to form a hot spot for fast ignition, such a profile of the REB may cause the increase of the growth rate of Weibel instability to compare with CP laser [4–7].

4 Diagnostic techniques and systems

We apply diagnostic techniques in many ways and set up a relatively integrated diagnostic system to measure physical experiments, such as, using the ninth beam to measure implosion dynamics, using the gated multi-framing camera and Wolter X-ray microscopes to diagnose radiation transport and imploding behavior, and so on.

The latest advances in the diagnostic techniques are using the dynamic Mach-Zehnder interferogram image of the saturated soft X-ray laser at wavelength 13.9 nm, which is produced by the nickel-like silver in hot plasma driven by Nd glass laser, to measure the plasma density (Fig. 10a), and also using Thomson scattering experiments (Fig. 10b) combined with other methods to obtain plasma temperature, non-local heat flow and the plasma expanding velocity from the pattern structure of the experimental pictures on SG-II [8].

5 Target fabrications

In addition to direct-drive capsules with glass shell and multi-layer plastic shell, the hohlraum targets in various shapes have been applied to experimentally study radiation transport, opacity, indirect-drive implosion dynamics, etc. (Fig. 11).

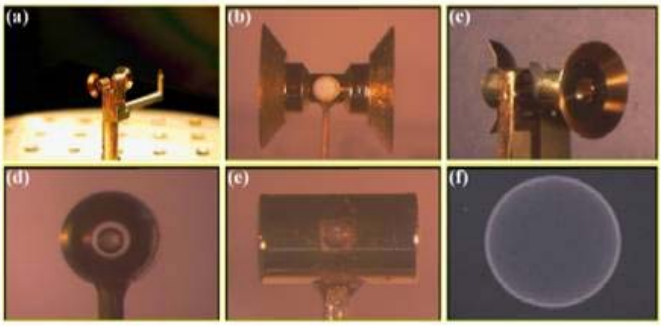

Fig. 11. Various configurations of the indirect-drive targets: (a) opacity target with two-point backlighting, (b) radiation transport target, (c) ablation target with two-point backlighting, (d, e) cylindrical hohlraum target (capsule inside), about $\phi = 800 \times 1600$ μm for SG-II experiments, (f) multi-layer (PS-PVA-CH) capsules, about $\phi = 300$–500 μm.

6 Summary and conclusion

In the past years, many important achievements were obtained in a series of experiments on SG-II to understand target physics; the numerical simulations using LARED series of codes can reproduce many experimental results and predict many new physical phenomena and provided the design parameters to construct SG-IIU, SG-III prototype and SG-III.

SG-IIU driver will serve for experiments in target physics beginning in 2007, and will couple with PW laser to investigate hot spot behavior of fast ignition.

SG-III prototype that began operating in 2005 will provide the use of both the technological platform for SG-III architecture and the physical experiment.

SG-III driver will be completed in about 2010 and be coupled with tens kJ PW lasers for fast ignition demonstration.

The ignition project was authorized. The architecture of SG-IV laser facility, National Ignition Driver, with laser energy output of about MJ for central ignition with moderate gain and fast ignition with high gain is being planned. China is going to be toward the goal of ignition and plasma burning in about 2020 and may advance to carry out it in about 2015 if fast ignition is favorable.

The authors would like to express their appreciation for the many people and the relevant institutions to diligently work under the ICF program in China. The work was supported by the National Hi-Tech Inertial Confinement Fusion Committee of China.

References

1. X.T. He et al., Inertial fusion energy research progress in China, in *6th Symposium On Current Trends in International Fusion Research: A Review*, 2005, `www.physicsessays.com`
2. W. Zheng, "Status of prototype for Shenguang-III laser facility," presentation at IFSA05
3. X.T. He, Jet-like long spike of ablative Rayleigh-Taylor instability, in *19th International Conference on Numerical Simulation of Plasma and 7th Asia Pacific Plasma Theory Conference*, July 12-15, 2005, Nara, Japan
4. C.Y. Zheng et al., Phys. Plasmas **12**, 044505 (2005)
5. B. Qiao et al., Phys. Plasmas **12**, 083102 (2005)
6. B. Qiao et al., Phys. Plasmas **12**, 053104 (2005)
7. H. Liu, X. T. He, S.G. Chen, Phys. Rev. E **69**, 066409 (2004)
8. Q.Z. Yu et al., Phys. Rev. E **71**, 046407 (2005)